

# We are IntechOpen, the world's leading publisher of Open Access books Built by scientists, for scientists

6,900

Open access books available

185,000

International authors and editors

200M

Downloads

Our authors are among the

154

Countries delivered to

TOP 1%

most cited scientists

12.2%

Contributors from top 500 universities



WEB OF SCIENCE™

Selection of our books indexed in the Book Citation Index  
in Web of Science™ Core Collection (BKCI)

Interested in publishing with us?  
Contact [book.department@intechopen.com](mailto:book.department@intechopen.com)

Numbers displayed above are based on latest data collected.  
For more information visit [www.intechopen.com](http://www.intechopen.com)



# Implantable Wireless Systems: A Review of Potentials and Challenges

*Amenah I. Kanaan and Ahmed M.A. Sabaawi*

## Abstract

With the current advancement in micro-and nano-fabrication processes and the newly developed approaches, wireless implantable devices are now able to meet the demand for compact, self-powered, wireless, and long-lasting implantable devices for medical and health-care applications. The demonstrated fabrication advancement enabled the wireless implantable devices to overcome the previous limitations of electromagnetic-based wireless devices such as the high volume due to large antenna size and to overcome the tissue and bone losses related to the ultrasound implantable devices. Recent state-of-the-art wireless implantable devices can efficiently harvest electromagnetic energy and detect RF signals with minimum losses. Most of the current implanted devices are powered by batteries, which is not an ideal solution as these batteries need periodic charging and replacement. On the other hand, the implantable devices that are powered by energy harvesters are operating continuously, patient-friendly, and are easy to use. Future wireless implantable devices face a strong demand to be linked with IoT-based applications and devices with data visualization on mobile devices. This type of application requires additional units, which means more power consumption. Thus, the challenge here is to reduce the overall power consumption and increase the wireless power transfer efficiency. This chapter presents the state-of-the-art wireless power transfer techniques and approaches that are used to drive implantable devices. These techniques include inductive coupling, radiofrequency, ultrasonic, photovoltaic, and heat. The advantages and disadvantages of these approaches and techniques along with the challenges and limitations of each technique will be discussed. Furthermore, the performance parameters such as operating distance, energy harvesting efficiency, and size will be discussed and analyzed to introduce a comprehensive comparison. Finally, the recent advances in materials development and wireless communication strategies, are also discussed.

**Keywords:** implantable wireless devices, wireless power transfer (WPT), coils, antennas, energy harvesting, SAR, link budget

## 1. Introduction

For more than 60 years, biomedical implantable device have been available. Earl Bakken designed and developed for the cardiac pacemaker in 1957, the first transistorized biomedical implanted device [1]. The most important issues of biomedical implants, namely patient safety and comfort, have been investigated. The result is a

reduction in energy consumption and an efficient transfer of energy to the implanted devices [2]. For implanted devices therefore, the transfer of wireless energy is an important issue. The power supply is a major technical challenge. If a battery is to be used due to its limited size and lifetime, an operation must be performed in a living body to swap the battery [3]. To prevent this invasive operation, a method of wireless transfer of power from outside the body should be developed [4]. The recent focus for biomedical applications is on wireless power transmission (WPT) due to its important benefits, such as facilitating implant surgery in which we avoid connected cable, improving rechargeable reliability, increasing healthcare workers and patients' safety [5]. The potential of WPT technology will introduce the new generation of safe and efficient medical devices [6]. The development of a system for nerve stimulation, cochlear aids, retinal implants, infusion pumps, pacemakers, cerebral pacemakers and others, has recently gained attention by wireless transfer of power (WPT). At the beginning of the 21st century, despite its high weight quality, limited lifetime, and chemical effects, certain applications for medical implanted devices (MID) were operated. The charging cables also had disadvantages and theoretically required a long time. In the early 21st century [7] Wireless Power Transfer Methods (WPT) received significant research interest in biomedical implants and neural prostheses. Patient tissue safety is one of the key factors in the WPT design for MIDs. The tissue safety is very much dependent on the body's EM constitutive parameters: the microwave power density, the frequency, tissue absorption and the sensitivity of the tissue. The effects of radio frequency waves cannot immediately be felt (and damages occur) by the patient as lower-frequency waves penetrate deeper into the tissue offering lower absorption. The relative allowability and conductivity of the human tissue decreases and increases with increasing frequencies, thereby increasing tissue absorption. Microwaves penetrate less and heat the tissue more easily at higher frequencies. The main tissue safety measure is the specific absorption rate for wireless power transmission applications for MIDs (SAR). When the electromagnetic wave travel through the tissue, it will penetrate the tissue but part of the wave will be absorbed by the tissue and get dissipated as heat. The interaction between the electromagnetic wave and the tissue depends on the dielectric properties of the tissue and the operating frequency. The amount of power absorbed by the tissue during the interaction is called specific absorption rate (SAR). The WPT proposed five methodologies: inductive transmission of energy (IPT) and capacitive transmission of power (CPT) and acoustic transmission of power (APT) in the neighborhood, as well as middle and remote field (RF) radiation [8]. The inductive links and the radio frequency are the two types of biomedical links (RF). A short-range communication channel that needs a coil antenna in the area of the output source is an inductive connection. On the other hand, the advantages of RF telemetry are reaching longer distances and improved information rates. In this regard, research is focused on implantable medical equipment connected to RF [9].

## 2. Implantable medical devices

Implantable medical devices have numerous functions that help to replicate human organ functions (**Table 1**). Implantable devices can be classified according to their functions as follows:

1. Implantable stimulator, like cardiac pacemaker, and defibrillator.
2. Implantable measuring system, like capsule endoscopy.

Class	Name	Function
Implantable simulator	Pacemaker	Make heart beat by electric current
	Brain pacemaker	Wake up vegetative state and treat depression
	Vibration control	Stimulate thalamic and deal with Parkinson's disease
Implantable measuring	Fixed	Measuring physiological and biochemistry parameters
Artificial organ	Capsule type	Diagnosing the digestive tract
	Heart	Repair or replace the cardiac structure
	Brain	Simulate the human brain
	Cochlea	For hearing rehabilitation
Implantable drug delivery		Give drug directly

**Table 1.**  
*Classification of implantable electronic devices.*

3. Implantable artificial organs, like artificial heart.

4. Implantable medical devices, like drug pump.

They have many other advantages, apart from the functions of these devices. It is possible to obtain test data without skin interference, which can reduce skin/device interaction. They can help cure diseases with external devices, for example Parkinson's and the normal organs such as heart, retina and cochlea can be changed with implanted devices. The most efficient approach is direct contact with organs.

3. Wireless power transfer (WPT)

Wireless Power Transfer Systems (WPT) can be classified as far- and near-field WPT systems. The WPT system in far field is divided into LASER, photoelectrical, RF and microwave whereas the inductive, magnetic and capacitive coupling methods are classified as the near-field. WPT is the main alternative to power-implantable devices by inductive connection and resonant connection [10]. The method is based on an antennas delivering RF power to a charging device. The wireless power transfer approaches are shown in **Figure 1**.

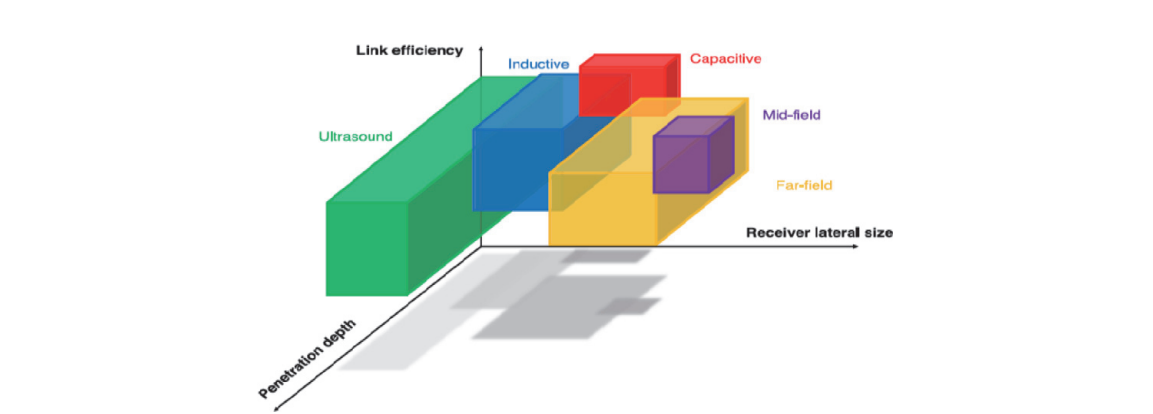


**Figure 1.**  
*The wireless power transfer methods [10].*

## 4. Near-field WPT methods

### 4.1 Capacitive coupling transfer

The capacitive coupling link approach is used to transfer data and power in short wireless communications to the implanted devices. The basis for this approach is two parallel plates which behave like condensers. The first plate is attached to the skin outside of the body; the second plate is implanted inside the body and attached as shown in **Figure 2** to the implanted device. The electric field is used as a carrier by the capacitive coupling to transfer data and power to the skin which acts as a dielectric divider between these two plates [11].

In **Figure 2**, the voltage transmission rate was analyzed as follows: The voltage of the  $V_{in}$  and the  $C_1$  and  $C_2$  between the implanted and the outside plates is the input capacitance equivalent,  $C_{in}$  is the implanted circuits' input capacitance and  $R_L$  is the equivalent "ac" of the loading system's resistance. The corresponding  $C_{eq}$  condensers are given

$$C_{eq} = C_1 + C_2 \quad (1)$$

Assuming  $C_{in} \ll C_{eq}$ , then

$$V_{out} = V_{in} \left[ \frac{R_L^2}{R_L^2 + X_{ceq}^2} + j \frac{R_L X_{eq}}{R_L^2 + X_{ceq}^2} \right] \quad (2)$$

and the voltage transfer rate is given by

$$\left| \frac{V_{out}}{V_{in}} \right| = \left( \frac{R_L^2}{R_L^2 + X_{ceq}^2} \right)^{1/2} \quad (3)$$

Therefore, when  $X_{Ceq} < R_L$ ,  $V_{out}$  is maximized. The main drawback of the method is that the tissue temperature of the plates can be increased, causing patient discomfort. The human body is also a non-magnetic material. Negligible losses in the magnetic field indicate that the electrical field is absorbed by human tissue [12].

### 4.2 Inductive coupling transfer

Inductive coupling transfer is now an attractive technology for the development of short communication biomedical applications. The magnetic coupling is used as the communication environment, common to techniques for radiofrequency

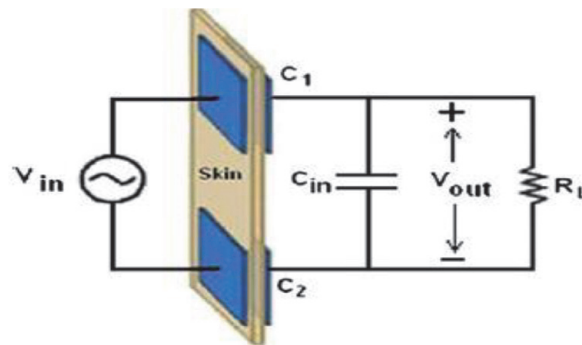


**Figure 2.**  
Simplified capacitive coupling transfer [12].

identification. The most popular way of transmitting power and data to passive implants [13] is the inductive power transfer between coupling coils, one on the implant and one outside the body on a reading device. As illustrated in **Figure 3**, the coil of the transmitter (TX) is placed adjacent to the skin and is a time variable magnetic field produced by a power source. This magnetic field induces an electromotive strength (EMF) inside the receiver (Rx) body that is processed using an RX system-based silicone rectifier [13]. In order to increase the PTE [14], the Rx coil should be tuned to the same working frequency as the Tx coil.

In passive systems, the connections have four categories for resonance: the SET (serial- to parallel) topology (SP), the serial-to-serial (SS) topology and the parallel-to-parallel (PP) topology as shown on **Figure 4**. In order to guarantee better efficiency in the transmission of power of the inductive connective transmission, both sides are tuned with the same resonant frequency  $f_0$ . In most cases, the principal circuit (reader) is tuned to series resonance, which gives the transmitter coil an impedance load which is almost always parallel to the secondary circuit and uses the LC circuit for driving a load of a not-linear corrective device [15].

The number of loops can be changed in practice based on wiring characteristics and coil form. A more practical approach consists of the measurement of inductance at construction and strange turns to achieve the specified inductance. However, a highly specialized and expensive inductance meter requires accurate measurement of inductance [15]. In practice, Equation (4) [16] can be used to calculate the resonance frequency  $f_0$ . Many formulas can be used to estimate the number of turns necessary to achieve a specific inductance  $L$ . For example, in **Table 2**, the (N)

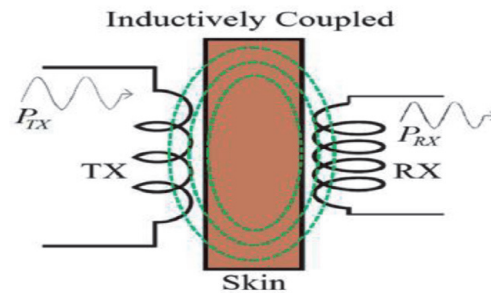


**Figure 3.**  
IC WPT system powered by alternative electromotive force (EMF). TX: transmitter coil. RX: receiving coil [13].

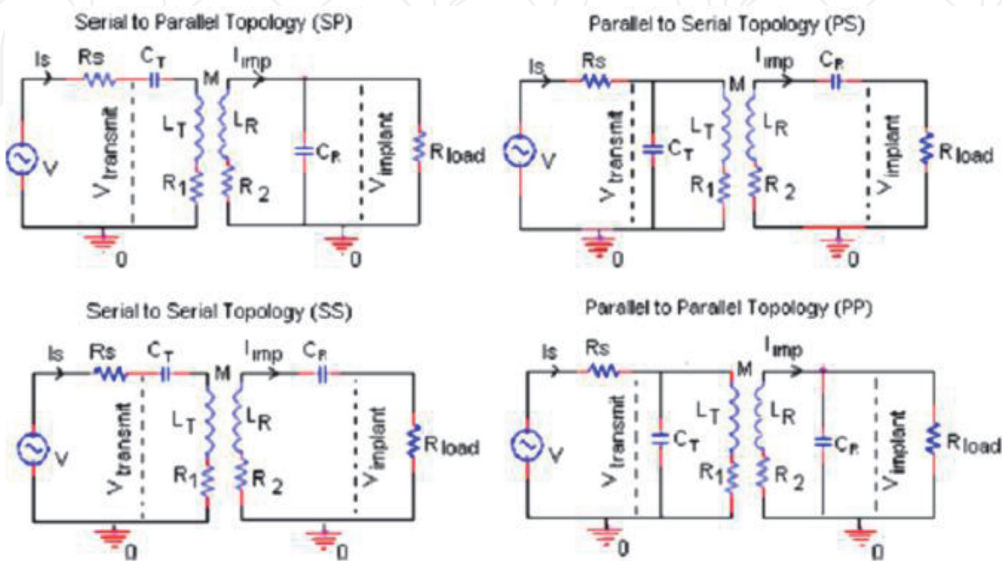


**Figure 4.**  
Inductive coupling with four possible resonance circuits [15].

Formulas	Reference
$L = N^2 R \mu_0 \mu_r \left( \ln \frac{8R}{a} - 0.2 \right)$	[17]
$L = \frac{r^2 N^2}{(2r + 2.8d) * 10^3}$	[18]
$L = \frac{0.3l(aN)^2}{6a + 9ha + b}$	[19]
$L = 2.9 \ln \left( \frac{9}{D} - K \right) N^{1.9}$	[20]

**Table 2.**

Formulas approximate the number of turns needed to achieve a given induction.

turnings on the radius of the loop (a), on height of the loop (h), on width of the loops (b), on width (d), on the loop radius (r) and on magnetic inductivity (L). But only approximations to ideal conditions [20] could be made in such equations.

$$K = \frac{M}{\sqrt{L_T L_R}} \quad (4)$$

The mutual inductivity (M) and coupling coefficient with  $L_T$  and  $L_R$ , as proposed by [21] are other parameters to be examined during inductive coupling design.

$$f_0 = \frac{1}{2\pi\sqrt{LC}} \quad (5)$$

The resistor  $R_1$  is the effective resistance series  $L_T$  with the SP topology given in **Figure 4** which shows the transferred spindle losses and the power amplifier's output resistance, whereas  $R_2$  is the effective  $L_R$  series resistance given in [21] and in [22].  $C_T$  and  $C_R$  capacitors are used on both sides of the link to create resonance.

The frequency of resonance ( $W_o$ ) of an LC tank may be calculated for both sides, as shown (6).

$$W_o = \frac{1}{\sqrt{L_T C_T}} = \frac{1}{\sqrt{L_R C_R}} \quad (6)$$

The quality factor (Q) in (7) is presented for the primary and secondary coils.

$$Q_1 = \frac{wL_T}{R_1} \text{ and } Q_2 = \frac{wL_R}{R_2} \quad (7)$$

The performance on both sides of the connection should be maximized for high efficiencies and this can occur when.

$$1 \ll K^2 Q_1 Q_2 = \frac{K^2 L_T}{L_R} * \frac{1}{R_2 C_T} \quad (8)$$

**Figure 5** shows total efficiency ( $K^2 Q_1 Q_2$ ) as a function of increasing efficiency with the increasing coupling and quality factor (9) [23].

$$\eta_{\max} = \frac{K^2 Q_1 Q_2}{\left(1 + \sqrt{K^2 Q_1 Q_2}\right)^2} \quad (9)$$

The resistance of implanted devices is another factor that directly affects overall efficiency (loaded case). The total efficiency is also raised proportionately with the load increases, depending on the implanted resistance proposed, according to (10) [24].

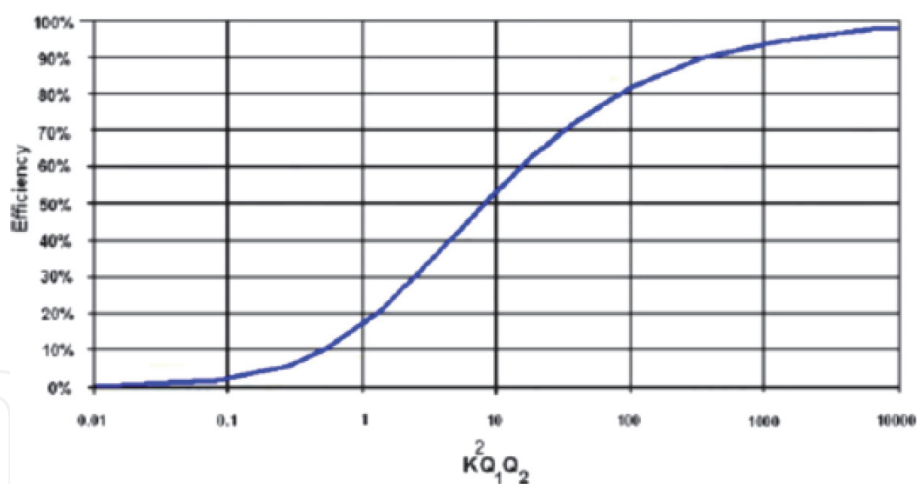


**Figure 5.**  
 Maximum achievable link efficiency as a function of  $(K_2Q_1Q_2)$  [23].

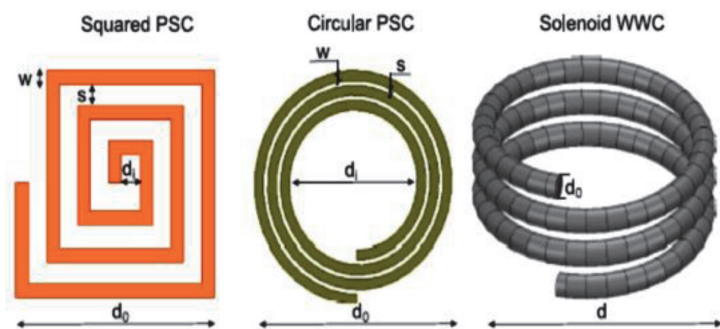


**Figure 6.**  
 Variants for the coil design: squared printed spiral coil (left), circular printed spiral coil (middle), and solenoid wire wound coil (right) [8].

$$\begin{aligned} \eta_{Total} &= \eta_T \eta_R \\ &= \frac{K^2 Q_1 Q_2^3 R_{LR} R_{Load}}{(K^2 Q_1 Q_2^3 R_{LR} R_{Load} + K^2 Q_1 Q_2 R_{Load}^2 + Q_2^4 Q_{LR}^2 + 2 Q_2^2 R_{LR} R_{Load} + R_{Load}^2)} \end{aligned} \tag{10}$$

The design of a coil with several possibilities, as outlined in **Figure 6**, is another relevant parameter. A first grade between printed spiral coils (PSC) and wound coils (WCs) [25] is established. A first classification is given. PSCs are characterized by high reliability and production ease, especially with micro and nano-production processes. However, PSCs have a lower quality factor than WWCs [20]. There are also different key parameters for the two geometries. For a PSC,  $d_0$  and  $d_i$  are the external and internal diameters of the spiral respectively,  $n$  is the number of turns where  $w$  and  $s$  are both the distance and the distance between them. For solenoid WWC, else,  $d$  is the diameter of the solenoid, constants during  $n$  rotations,  $l$  is the length of the driver,  $d_0$  is the diameter of the wiring and  $p$  is the twisting pitch [8].

### 4.3 Magnetic resonance coupling

As illustrated in **Figure 7**, magnet resonance coupling is based on evanescent wave-coupling which generates and transfers electric energy through various or varying magnetic fields between the two resonant spins. As two resonant coils are strongly coupled with the same resonant frequency, high efficacy can be achieved. The advantage of the magnetic resonance connection are also immunity to the

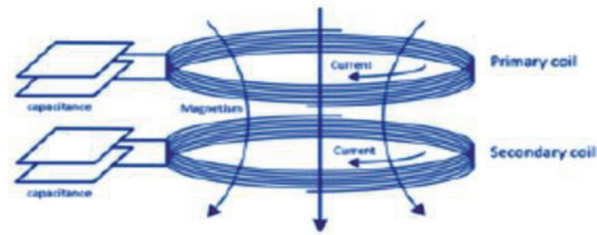


**Figure 7.**  
Magnetic resonance coupling [26].

surrounding environment and the need for a free space transfer [26]. The quality factors are normally high, because magnetic resonance coupling usually works within the megahertz range. The high quality factor helps to mitigate a sharp reduction in connection effectiveness and thus loading efficiency, by increasing the loading distance. As a result, it is possible to extend the effective transmission power distance to meters [27].

With the declaration of the Wireless Power Consortium (WPC) on extending the transfer distance from 5 mm to 40 mm in 2012, new research works are expected to focus on new magnetic winding schemes and configurations [28]. Based on the new developments in improving the transfer distance, a new planar design would be able to charge the devices on desks and tables. To address the poor transfer efficiency defects of a two-coil energy transfer mechanism, as considered in [29], midrange WPT techniques, such as relay resonators (**Figure 8a**), four coils (**Figure 8b**), U coils (**Figure 8c**), domino coils (**Figure 8d**), array coils (**Figure 8e**), and dipole coils (**Figure 8f**) are proposed in previous studies and fused into future planar WPT chargers with increased distances or air gaps. Based on these studies, the transfer distances were 20, 60, 100, 180 (for seven resonator coils), 20, and 500 cm respectively) [30]. Each configurations have superior performance

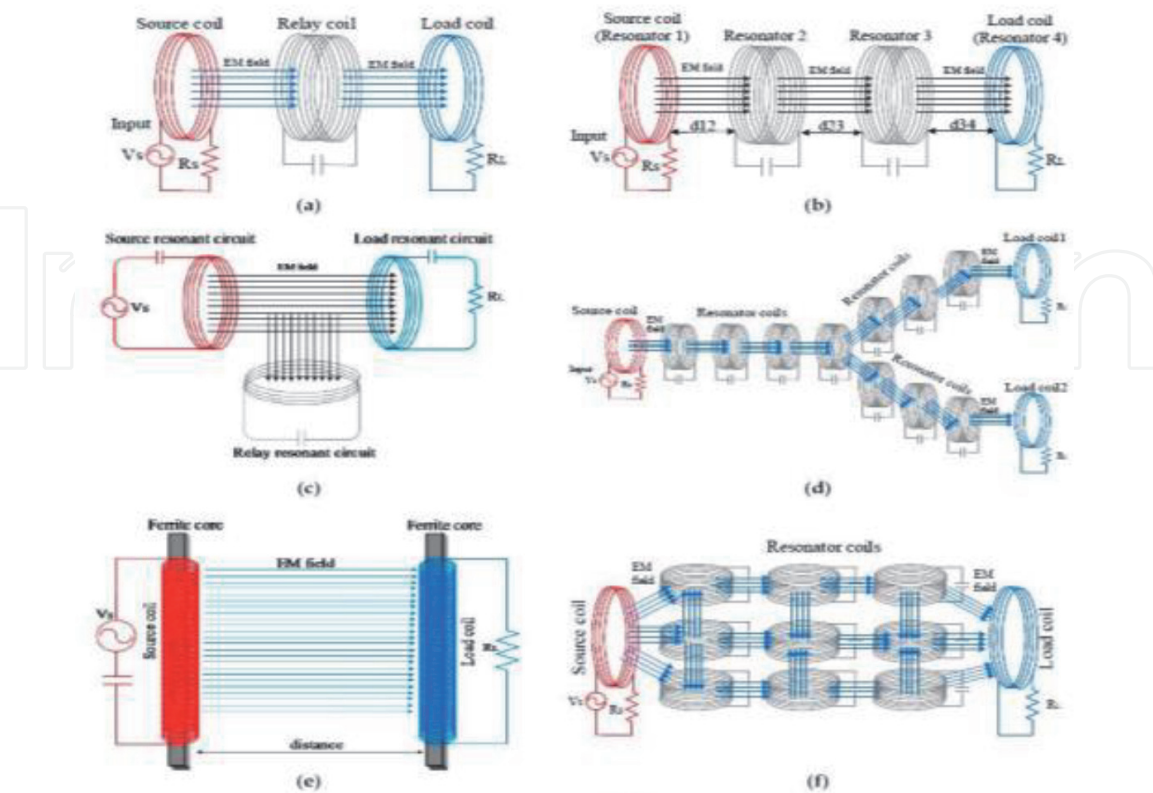


**Figure 8.**  
Different WPT mechanisms: (a) relay coil; (b) four coils; (c) U-coil; (d) domino coils; (e) dipole coils; and (f) array coils [30].

characteristics than the NRIC in several aspects: (a) better impedance matching capability to optimize the system power transfer, (b) higher Q-factor enabled by the primary and secondary coils, which can compensate for the sharp decline of PTE caused by the reduced coupling coefficient due to the increasing separation distance and (c) higher bandwidth of operation [31].

5. Far-field electromagnetic systems

As mentioned earlier in this chapter, the main issue in the implanted devices is the battery due to their bulkiness and limited life time, which make them not suitable for long term applications. Thus, it is necessary to power up the implanted device wirelessly through one of the wireless power transfer techniques (i.e. inductive coupling or far-field). Inductive coupling method is used in most conventional wireless power transmission systems, where the transfer of power depends on the coupling between pair of adjacent coils. The main issue in this method is the fact that low frequency electromagnetic waves for power transmission require relatively large coils. On the other hand, wireless implanted devices need to be compact as much as possible for making them allowable to be implanted at different parts of the body (system scalability) and to improve resolution of received signals. This issue can be addressed by utilizing RF systems in order to miniaturize the implanted device and improve the wireless communication link. The amount of harvested power in the RF systems is limited to few hundreds of  $\mu\text{W}$  due to the regulation of transmitted power keeping it under the safe level. It is hence needed to have an efficient antenna to receive the signal and efficient rectifying and power management process in order to provide enough power for high-performance implanted biomedical devices. **Figure 9** illustrates a block diagram of power harvesting platform for a wirelessly powered implanted device [32]. The system design employs an integrated on-chip loop antenna. The antenna passes the received power to a multi-stage rectifier to convert it into DC voltage, which is then passed to the power management unit. It is worth mentioning here that double-gate CMOS transistors can be used and operated at deep threshold region in order to minimize the power consumption and reduce the leakage current.

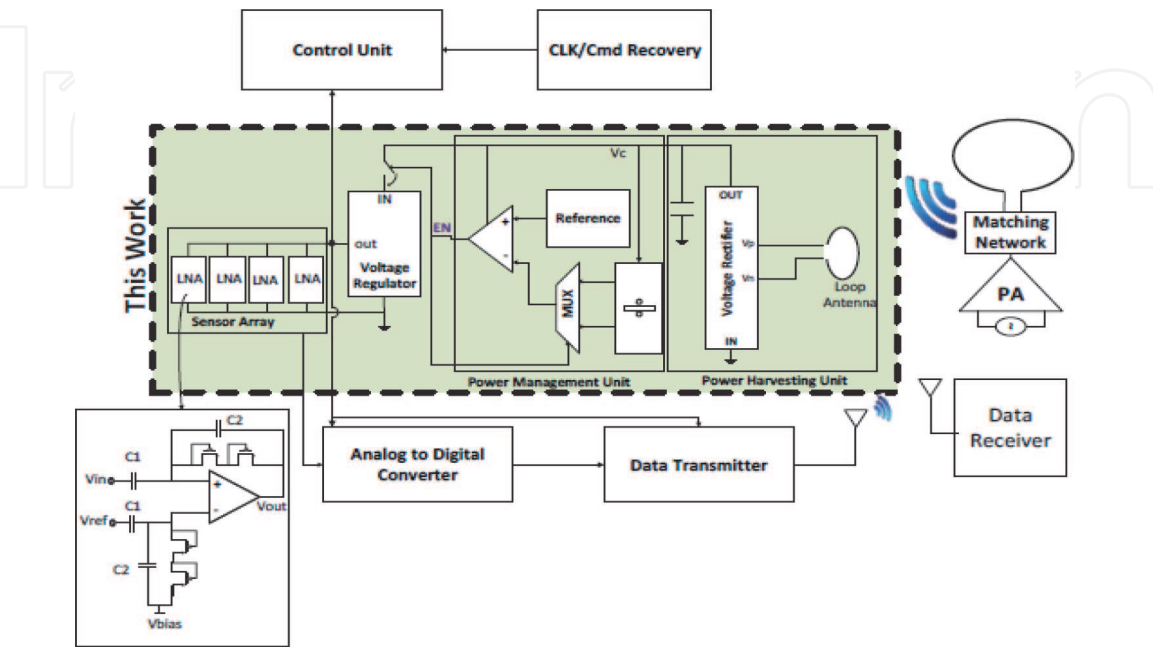


**Figure 9.**  
Block diagram of power harvesting platform for a wirelessly powered implanted device [32].

## 5.1 Specific absorption rate (SAR)

When the electromagnetic wave travel through the tissue, it will penetrate the tissue but part of the wave will be absorbed by the tissue and get dissipated as heat. The interaction between the electromagnetic wave and the tissue depends on the dielectric properties of the tissue and the operating frequency. The amount of power absorbed by the tissue during the interaction is called specific absorption rate (SAR), which can be expressed by the electric field ( $E$ ) of the incident wave as follows:

$$SAR = \frac{\sigma}{2\rho} |E|^2 \quad (11)$$

where  $\sigma$  and  $\rho$  are the tissue conductivity and volume density, respectively. When working at near field, the temperature of the tissue will be increased due to the dissipation of EM at the tissue interface. The rate of temperature change ( $\Delta T$ ) measured in ( $^{\circ}\text{C}$ ) depends mainly on SAR and can be given as:

$$\frac{\Delta T}{\Delta t} = \frac{(SAR + P_m - P_c - P_b)}{h_c} \quad (12)$$

where  $P_m$ ,  $P_c$  and  $P_b$  are the metabolic heating rates; and  $h_c$  is the tissue heat capacity.

There are two SAR standards enforced by IEEE to determine the maximum allowable power for safe interaction between the electromagnetic wave and the tissue without causing any damage or harmful interaction. These standards are IEEE C95.1-1999 standard ( $SAR_{1g} \leq 1.6 \text{ W/kg}$ ) and IEEE C95.1-2005 standard ( $SAR_{10g} \leq 2 \text{ W/kg}$ ).

## 5.2 Impact of tissue type on antenna performance

As mentioned earlier in this chapter, interaction of the electromagnetic wave with the tissue depends on the operating frequency and the dielectric properties. Thus, it is expected that the antenna of the implanted device behaves differently based on which part of the body the device is implanted as well as depending on the frequency of the EM. In [33], a dual band flower-shaped antenna is proposed for wireless implanted devices as shown in **Figure 10**.

The performance of the antenna at different part of the body was recorded for both frequency bands as summarized in **Table 3** below. It is clearly observed that the performance of the antenna is changed when placed at different parts of the body. It was also noticed that the bandwidth is higher at 2.45 GHz frequency band compared with 928 MHz, however, the gain was smaller. Thus, there is a tradeoff between the gain and the bandwidth depends on the application of the wireless implanted device.

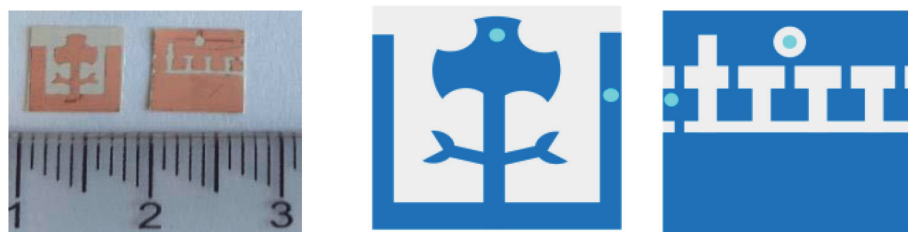


**Figure 10.**  
The proposed flower-shaped antenna [33].

	Homogenous phantom		Head		Stomach		Small intestine		Measured	
Frequency	928 MHz	2.45 GHz	928 MHz	2.45 GHz	928 MHz	2.45 GHz	928 MHz	2.45 GHz	928 MHz	2.45 GHz
BW (MHz)	197.6	245.3	231.1	600	190	204	249.5	502.5	180	365.4
G (dBi)	-28.44	-25.65	-33.67	-29	-27.69	-25.58	-29.74	-22.39	-28.94	-26.37

**Table 3.**  
Summarized performance parameters (bandwidth and gain) of the proposed flower-shaped antenna [33].

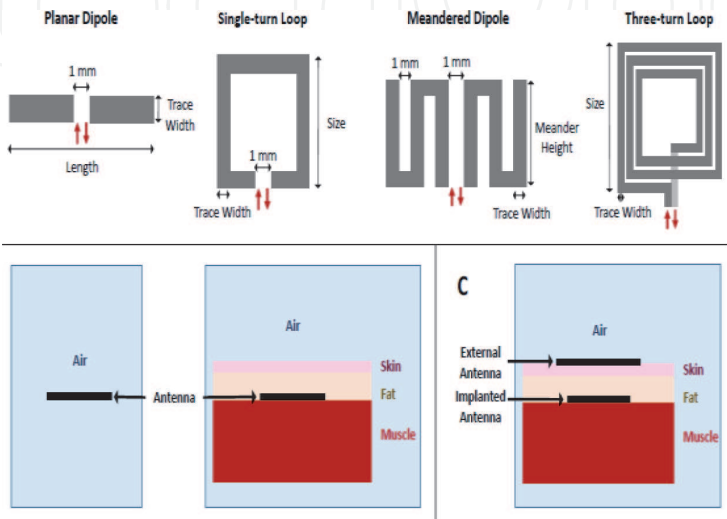


**Figure 11.**  
The proposed dipole and loop UHF antennas [34].

The antenna type play an important role in the wireless implanted system. Thus, it is important to study different antenna types at different parts of the human body and compare the performance. In [34], a comparison is made between dipole and loop antennas, where several dipole and loop antennas were designed as shown in **Figure 11**.

Recent study showed that the loop topologies provide higher gain than dipole topologies with achieving miniaturized size, while dipole antennas exhibits better impedance matching properties [34]. In addition, the dipole antennas showed a better ability to increase the gain and less sensitivity changes in tissue structure. The variation of antenna gain at different parts of the body is plotted in **Figure 12** [34] for both topologies (i.e. dipole and loop).

Another studies investigated the impact of tissue location on the return loss of the antenna at high frequencies as shown in **Figure 13** [35]. It was observed that the resonant frequency and the bandwidth can be changed by placing the antenna at another body part such as hand, heart, chest and head.

5.3 Muti-band antennas for wireless implanted devices

In wireless implanted devices, the antenna plays a key role in managing the communication process as well as the transfer of power. Hence, it is a multi-task process that require more than one frequency band operating simultaneously. For example, a frequency band is needed for biotelemetry and another one for power transfer. In addition, a higher frequency might be needed for wakeup controller. Since the implanted device is needed to be miniaturized, it is preferable to employ one antenna that can operate efficiently at more than one frequency.

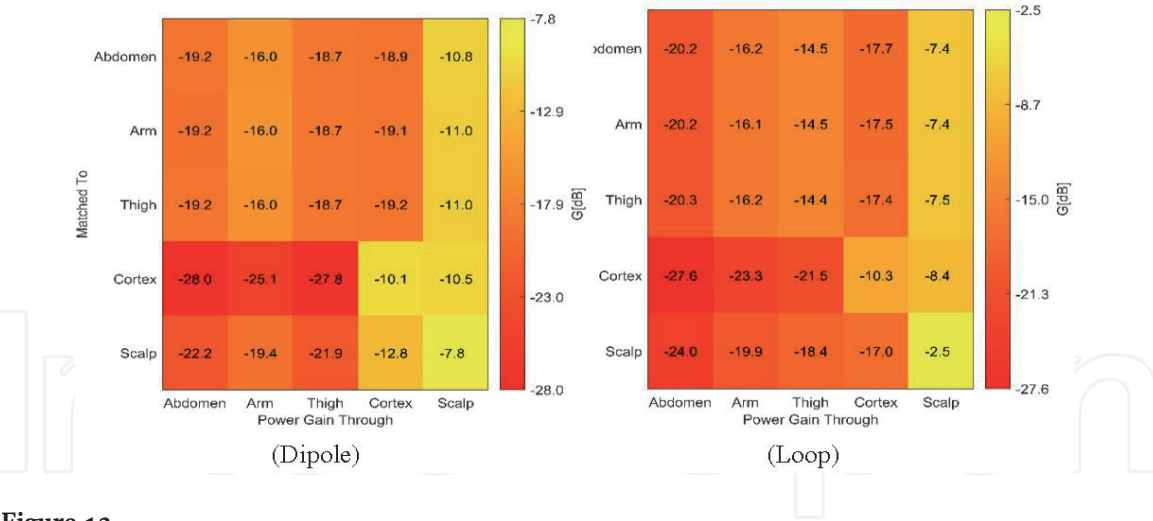


**Figure 12.** Power gain ( $G$ ) of both topologies at different tissue locations [34].

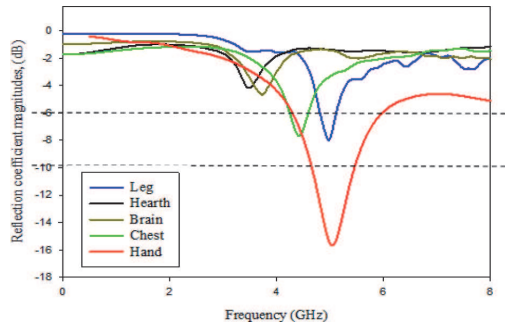


**Figure 13.** Variation of resonant frequency and bandwidth at different parts of human body [35].

Several recent studies [36, 37] attempted to address the multi-band issue by designing a dual- or triple-band antennas. In [37], a dual band antenna operating at 915 MHz and 2.45 GHz is designed and fabricated for scalp-implanted devices. The fabricated meandered line antenna and the experimental setup is shown in **Figure 14**. For validation, normally the measurements must of antennas for wireless implanted devices are carried out in saline solution. **Figure 15** presents the simulated and measured return loss of the designed antenna. It is worth mentioning that the link margin decreases with increasing the transmission range, where the highest bit rate undergoes larger loss as shown in **Figure 16**.

Another compact multi-band antenna is proposed in [37]. The implemented antenna exhibits triple resonance behavior due to the employment of spiral structure. The antenna can be operated at 433.1–434.8 MHz, 1520–1693 MHz and 2400–2483.5 MHz. The fabricated triple-band spiral antenna and the experimental set up is depicted in **Figure 17**. In addition, **Figure 18** illustrates the SAR values for all frequency bands.

Some studies in literature has proposed different frequency band [38]. **Figure 19** shows the return loss of the designed antenna showing the three resonant frequencies and the bandwidth for each band.

5.4 Employing RFID antennas in wireless implanted devices

Some studies proposed the use of near-field inductively coupled implanted devices operating at low frequencies with two antennas (implanted and wearable);

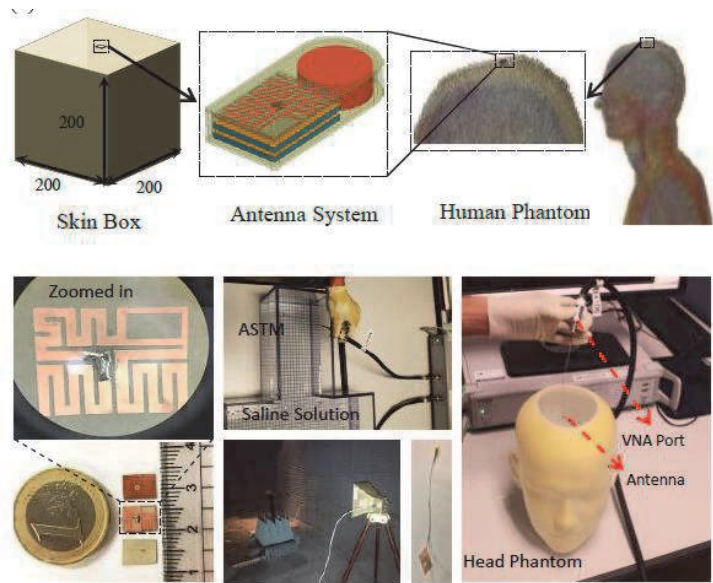


Figure 14.  
Fabricated antenna and experimental set up [36].

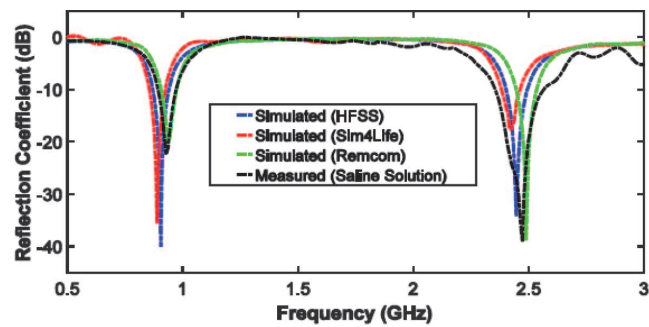


Figure 15.  
Simulated and measured return loss [36].

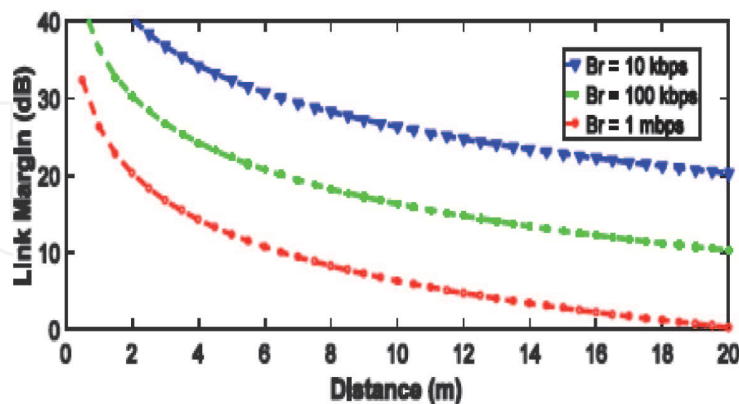
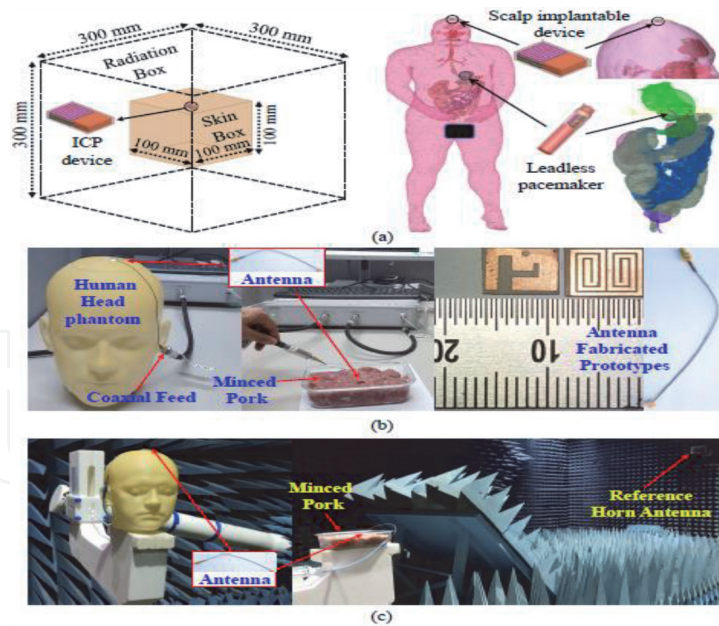


Figure 16.  
Variation of link margin with communication distance for different bit rates [36].

and an additional far-field antenna for the off-body data transmission system. RFID approach is suggested in [39], where the implant part carries a backscattering microsystem. On the other hand, the wearable antenna (outer ring) serves as the radiating part for the off-body data communication as shown in **Figure 20**.

One of the biggest challenges of the far-field antennas that are used in implanted devices is the large size of the antenna, which should be proportional to the wavelength of the electromagnetic waves. In this application, the implanted device needs



**Figure 17.**  
The Fabricated triple-band spiral antenna and experimental set up [37].



**Figure 18.**  
Simulated averaged SAR surface (top row) and coronal (bottom row) distributions over 1-g of tissue in an anatomical human head model [37].

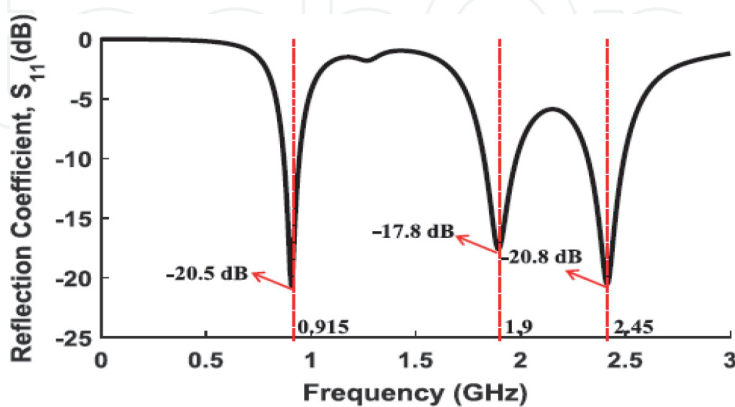


**Figure 19.**  
Simulated and measured return loss for the designed triple-band antenna [38].

to as small as possible, thus, it is important to design miniaturized antennas with acceptable efficiency. To address this issue, a compact electromagnetic antenna array with dimensions around 200  $\mu\text{m}$  can be utilized as reported in [40]. The proposed antenna system can harvest electromagnetic energy to power up the RFID

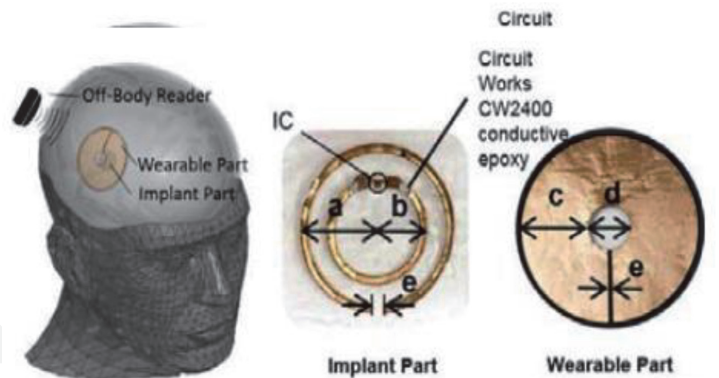


**Figure 20.**  
*Implantable and wearable antenna prototypes for brain RFID system [39].*

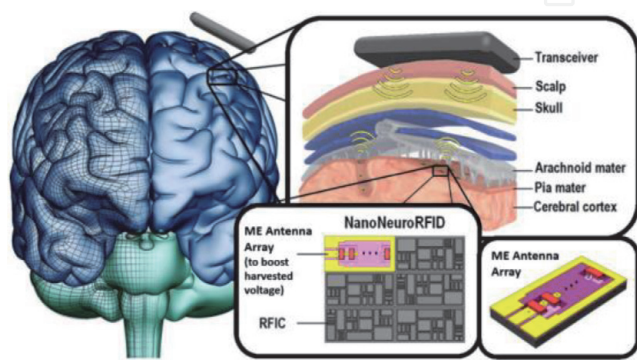


**Figure 21.**  
*Wireless implantable NanoNeuroRFID system reported in [39].*

system. In addition, the antenna array can sense the neuronal magnetic fields. The overall wireless implantable NanoNeuroRFID system is shown in **Figure 21**.

5.5 Antenna alignment in wireless implantable devices

One of the common challenges in wireless implanted systems is the misalignment in radiation direction and polarization. This issue can be easily addressed by increasing the transmitted power, however, there are safety risks limiting the amount of incident power. Utilizing circularly polarized antennas can only solve the problem of polarization misalignment keeping the radiation direction unaddressed. Thus, researcher paid significant efforts to design a universal solution for the aforementioned issues. One of the solutions is proposed in [40], where the harmonics yielded by the nonlinearity of rectifiers were exploited to align the

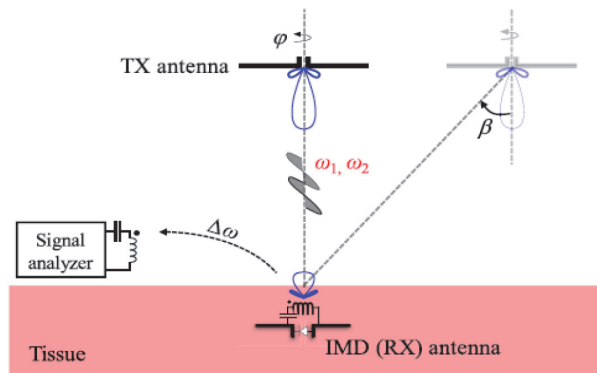


**Figure 22.**  
*Proposed intermodulation-based system for addressing the misalignment [40].*

transmitting and receiving antennas effectively. In this approach, two-tone (2T) waveform excitation is utilized to improve the rectification as well as to generate intermodulation as shown in **Figure 22**.

## 6. Summary


This chapter highlighted the basic structure of wireless implanted devices and focused on the various methods that are utilized in designing implanted devices. Near-field coupling techniques such as capacitive, inductive and magnetic resonance were discussed in details. The main focus in this chapter was on the employment far-field antennas, were the impact on the human body on the antenna performance. Different types of antennas were discussed and analyzed as well as the allowed safe power levels. The utilizing of RFID technology in wireless implanted device were presented in discussed. Finally, new alignment techniques for the antennas of implanted devices were introduced.

### Author details

Amenah I. Kanaan\* and Ahmed M.A. Sabaawi  
College of Electronics Engineering, Ninevah University, Mosul, Iraq

\*Address all correspondence to: [amina.edrees@gmail.com](mailto:amina.edrees@gmail.com)

### IntechOpen

© 2021 The Author(s). Licensee IntechOpen. This chapter is distributed under the terms of the Creative Commons Attribution License (<http://creativecommons.org/licenses/by/3.0>), which permits unrestricted use, distribution, and reproduction in any medium, provided the original work is properly cited. 

## References

- [1] D. J. Rhees, "From Frankenstein to the pacemaker," *IEEE Engineering in Medicine and Biology Magazine*, vol. 28, no. 4, pp. 78–84, Jul. 2009, doi: 10.1109/MEMB.2009.933571.
- [2] S. Mandal and R. Sarpeshkar, "Power-Efficient Impedance-Modulation Wireless Data Links for Biomedical Implants," *IEEE Transactions on Biomedical Circuits and Systems*, vol. 2, no. 4, pp. 301–315, Dec. 2008, doi: 10.1109/TBCAS.2008.2005295.
- [3] M. A. Hannan, S. M. Abbas, S. A. Samad, and A. Hussain, "Modulation Techniques for Biomedical Implanted Devices and Their Challenges," *Sensors*, vol. 12, no. 1, pp. 297–319, Dec. 2011, doi: 10.3390/s120100297.
- [4] K. H. Jung, Y. H. Kim, J. Kim, and Y. J. Kim, "Wireless power transmission for implantable devices using inductive component of closed magnetic circuit," *Electron. Lett.*, vol. 45, no. 1, p. 21, 2009, doi: 10.1049/el:20092241.
- [5] R. A. Bercich, D. R. Duffy, and P. P. Irazoqui, "Far-Field RF Powering of Implantable Devices: Safety Considerations," *IEEE Trans. Biomed. Eng.*, vol. 60, no. 8, pp. 2107–2112, Aug. 2013, doi: 10.1109/TBME.2013.2246787.
- [6] Z. Chen, H. Sun, and W. Geyi, "Maximum Wireless Power Transfer to the Implantable Device in the Radiative Near-Field," *Antennas Wirel. Propag. Lett.*, pp. 1–1, 2017, doi: 10.1109/LAWP.2017.2677739.
- [7] M. A. Hussain, S. K. Gharghan, and H. Q. Hamood, "Design and Implementation of Wireless Low-Power Transfer for Medical Implant Devices," *IOP Conf. Ser.: Mater. Sci. Eng.*, vol. 745, p. 012087, Mar. 2020, doi: 10.1088/1757-899X/745/1/012087.
- [8] G. L. Barbruni, P. M. Ros, D. Demarchi, S. Carrara, and D. Ghezzi, "Miniaturised Wireless Power Transfer Systems for Neurostimulation: A Review," *IEEE Trans. Biomed. Circuits Syst.*, vol. 14, no. 6, pp. 1160–1178, Dec. 2020, doi: 10.1109/TBCAS.2020.3038599.
- [9] C. Liu, Y.-X. Guo, and S. Xiao, "A Review of Implantable Antennas for Wireless Biomedical Devices," p. 11.
- [10] R. Shadid and S. Noghanian, "A Literature Survey on Wireless Power Transfer for Biomedical Devices," *International Journal of Antennas and Propagation*, vol. 2018, pp. 1–11, 2018, doi: 10.1155/2018/4382841.
- [11] M. A. Hannan, S. Mutashar, S. A. Samad, and A. Hussain, "Energy harvesting for the implantable biomedical devices: issues and challenges," *BioMed Eng OnLine*, vol. 13, no. 1, p. 79, 2014, doi: 10.1186/1475-925X-13-79.
- [12] J. Riistama et al., "Wireless and inductively powered implant for measuring electrocardiogram," *Med Bio Eng Comput*, vol. 45, no. 12, pp. 1163–1174, Dec. 2007, doi: 10.1007/s11517-007-0264-0.
- [13] P. T. Theilmann and P. M. Asbeck, "An Analytical Model for Inductively Coupled Implantable Biomedical Devices With Ferrite Rods," *IEEE Trans. Biomed. Circuits Syst.*, vol. 3, no. 1, pp. 43–52, Feb. 2009, doi: 10.1109/TBCAS.2008.2004776.
- [14] S. R. Khan, S. K. Pavuluri, G. Cummins, and M. P. Y. Desmulliez, "Wireless Power Transfer Techniques for Implantable Medical Devices: A Review," *Sensors*, vol. 20, no. 12, p. 3487, Jun. 2020, doi: 10.3390/s20123487.
- [15] J. O. Bird, *Electrical Circuit Theory and Technology*. Routledge, 2007.

- [16] J. A. Svoboda and R. C. Dorf, *Introduction to Electric Circuits*. John Wiley and Sons, 2013.
- [17] H. L. Chan, K. W. E. Cheng, and D. Sutanto, "A simplified Neumann's formula for calculation of inductance of spiral coil," pp. 69–73, Jan. 2000, doi: 10.1049/cp:20000222.
- [18] G. Mykolaitis, A. Tamaševičius, S. Bumelienė, A. Baziliauskas, and E. Lindberg, "Two-Stage Chaotic Colpitts Oscillator for the UHF Range," *ELEKTRON ELEKTROTECH*, vol. 53, no. 4, Art. no. 4, Apr. 2004, Accessed: May 01, 2021. [Online]. Available: <https://eejournal.ktu.lt/index.php/elt/article/view/10923>.
- [19] B. Lenaerts and R. Puers, "Omnidirectional Coupling," in *Omnidirectional Inductive Powering for Biomedical Implants*, B. Lenaerts and R. Puers, Eds. Dordrecht: Springer Netherlands, 2009, pp. 119–138.
- [20] U.-M. Jow and M. Ghovanloo, "Design and Optimization of Printed Spiral Coils for Efficient Inductive Power Transmission," in *2007 14th IEEE International Conference on Electronics, Circuits and Systems*, Dec. 2007, pp. 70–73, doi: 10.1109/ICECS.2007.4510933.
- [21] W. Liu et al., "Implantable biomimetic microelectronic systems design," *IEEE Engineering in Medicine and Biology Magazine*, vol. 24, no. 5, pp. 66–74, Sep. 2005, doi: 10.1109/MEMB.2005.1511502.
- [22] R. R. Harrison, "Designing Efficient Inductive Power Links for Implantable Devices," in *2007 IEEE International Symposium on Circuits and Systems*, May 2007, pp. 2080–2083, doi: 10.1109/ISCAS.2007.378508.
- [23] M. W. Baker and R. Sarpeshkar, "Feedback Analysis and Design of RF Power Links for Low-Power Bionic Systems," *IEEE Transactions on Biomedical Circuits and Systems*, vol. 1, no. 1, pp. 28–38, Mar. 2007, doi: 10.1109/TBCAS.2007.893180.
- [24] R.-F. Xue, K.-W. Cheng, and M. Je, "High-Efficiency Wireless Power Transfer for Biomedical Implants by Optimal Resonant Load Transformation," *IEEE Transactions on Circuits and Systems I: Regular Papers*, vol. 60, no. 4, pp. 867–874, Apr. 2013, doi: 10.1109/TCSI.2012.2209297.
- [25] A. Ibrahim and M. Kiani, "A Figure-of-Merit for Design and Optimization of Inductive Power Transmission Links for Millimeter-Sized Biomedical Implants," *IEEE Transactions on Biomedical Circuits and Systems*, vol. 10, no. 6, pp. 1100–1111, Dec. 2016, doi: 10.1109/TBCAS.2016.2515541.
- [26] L. Chen, S. Liu, Y. C. Zhou, and T. J. Cui, "An Optimizable Circuit Structure for High-Efficiency Wireless Power Transfer," *IEEE Transactions on Industrial Electronics*, vol. 60, no. 1, pp. 339–349, Jan. 2013, doi: 10.1109/TIE.2011.2179275.
- [27] M. D. B. Ahire and D. V. J. Gond, "Wireless Power Transfer System for Biomedical Application: A Review," p. 6, 2017.
- [28] S. Y. Hui, "Planar Wireless Charging Technology for Portable Electronic Products and Qi," *Proceedings of the IEEE*, vol. 101, no. 6, pp. 1290–1301, Jun. 2013, doi: 10.1109/JPROC.2013.2246531.
- [29] S. Y. R. Hui, W. Zhong, and C. K. Lee, "A Critical Review of Recent Progress in Mid-Range Wireless Power Transfer," *IEEE Transactions on Power Electronics*, vol. 29, no. 9, pp. 4500–4511, Sep. 2014, doi: 10.1109/TPEL.2013.2249670.
- [30] H. Jawad, R. Nordin, S. Gharghan, A. Jawad, and M. Ismail, "Energy-

Efficient Wireless Sensor Networks for Precision Agriculture: A Review,” *Sensors*, vol. 17, no. 8, p. 1781, Aug. 2017, doi: 10.3390/s17081781.

[31] S. R. Khan, S. K. Pavuluri, and M. P. Y. Desmulliez, “Accurate Modeling of Coil Inductance for Near-Field Wireless Power Transfer,” *IEEE Transactions on Microwave Theory and Techniques*, vol. 66, no. 9, pp. 4158–4169, Sep. 2018, doi: 10.1109/TMTT.2018.2854190.

[32] H. Rahmani and A. Babakhani, “A wireless power receiver with an on-chip antenna for millimeter-size biomedical implants in 180 nm SOI CMOS,” in 2017 IEEE MTT-S International Microwave Symposium (IMS), Honolulu, HI, USA, Jun. 2017, pp. 300–303, doi: 10.1109/MWSYM.2017.8059103.

[33] F. Faisal and H. Yoo, “A Miniaturized Novel-Shape Dual-Band Antenna for Implantable Applications,” *IEEE Trans. Antennas Propagat.*, vol. 67, no. 2, pp. 774–783, Feb. 2019, doi: 10.1109/TAP.2018.2880046.

[34] K. N. Bocan, M. H. Mickle, and E. Sejdic, “Tissue Variability and Antennas for Power Transfer to Wireless Implantable Medical Devices,” *IEEE J. Transl. Eng. Health Med.*, vol. 5, pp. 1–11, 2017, doi: 10.1109/JTEHM.2017.2723391.

[35] N. H. Ramli, H. Jaafar, and Y. S. Lee, “Numerical Investigation of a Chip Printed Antenna Performances for Wireless Implantable Body Area Network Applications,” *IOP Conf. Ser.: Mater. Sci. Eng.*, vol. 318, p. 012047, Mar. 2018, doi: 10.1088/1757-899X/318/1/012047.

[36] S. A. A. Shah and H. Yoo, “Scalp-Implantable Antenna Systems for Intracranial Pressure Monitoring,” *IEEE Trans. Antennas Propagat.*, vol. 66, no. 4, pp. 2170–2173, Apr. 2018, doi: 10.1109/TAP.2018.2801346.

[37] I. A. Shah, M. Zada, and H. Yoo, “Design and Analysis of a Compact-Sized Multiband Spiral-Shaped Implantable Antenna for Scalp Implantable and Leadless Pacemaker Systems,” *IEEE Trans. Antennas Propagat.*, vol. 67, no. 6, pp. 4230–4234, Jun. 2019, doi: 10.1109/TAP.2019.2908252.

[38] M. Zada and H. Yoo, “A Miniaturized Triple-Band Implantable Antenna System for Bio-Telemetry Applications,” *IEEE Trans. Antennas Propagat.*, vol. 66, no. 12, pp. 7378–7382, Dec. 2018, doi: 10.1109/TAP.2018.2874681.

[39] S. Ma, M. W. A. Khan, L. Sydänheimo, L. Ukkonen, and T. Björninen, “Implantable Sensors and Antennas for Wireless Brain Care,” in 2018 2nd URSI Atlantic Radio Science Meeting (AT-RASC), May 2018, pp. 1–2, doi: 10.23919/URSI-AT-RASC.2018.8471421.

[40] M. Zaeimbashi et al., “NanoNeuroRFID: A Wireless Implantable Device Based on Magnetoelectric Antennas,” *IEEE J. Electromagn. RF Microw. Med. Biol.*, vol. 3, no. 3, pp. 206–215, Sep. 2019, doi: 10.1109/JERM.2019.2903930.